Diversity Combining Scheme for Time-Varying STBC NGSO Multi-Satellite Systems

Vibhum Singh, *Member, IEEE*, Geoffrey Eappen, *Member, IEEE*, Wallace A. Martins, *Senior Member, IEEE*, Rakesh Palisetty, *Member, IEEE*, Carlos Luis Marcos Rojas, *Graduate Student Member, IEEE* Jorge Luis Gonzalez-Rios, *Member, IEEE*, Juan A. Vásquez-Peralvo, *Member, IEEE*, Jevgenij Krivochiza, *Member, IEEE*, Juan Carlos Merlano-Duncan, *Senior Member, IEEE*, Luis Garces Socarras, *Member, IEEE*, Symeon Chatzinotas, *Fellow, IEEE*, Björn Ottersten, *Fellow, IEEE*

***Abstract*—Current trends in non-geostationary orbit (NGSO) satellite communications pose the challenge of attaining high spectral efficiency with low-complexity user terminals (UTs). In this context, this letter investigates the downlink/forward transmission of linear space-time block coded (STBC) signals through multiple geographically distributed NGSO satellites. As such, by combining the signals through multiple satellites, STBC provides a diversity advantage, which helps in combating the adverse effects of fading and interference at the UT. The main challenge of implementing such a scheme is the lack of time synchronization and the interference effect through a multi-satellite system toward the UT. To address this issue, we propose a digital receiver structure with multiple branches specifically designed to lock onto each satellite of the multi-satellite system, thus providing a solution for simple UT without requiring additional complexity in terms of radio-frequency components. Herein, we consider the zero-forcing (ZF) based diversity combining scheme while deriving the signal-to-interference-plus-noise ratio (SINR) expression at UT. Our results demonstrate the SINR improvement brought by the ZF combiner.**

***Index Terms*—Diversity combining, non-geostationary orbit, satellite communication systems, space-time block coding, time misalignment, zero-forcing.**

I. Introduction

SATELLITES with their wide coverage can enable "any-time/anywhere access" at affordable costs, thereby staking a claim in future wireless networks [1]. In particular, the space-based component can substantially augment the fifth-generation (5G) and beyond service capabilities. These enhancements are enabled by the satellite's inherent structure that supports envisioned multimedia traffic growth and ubiquitous coverage. These, in turn, will be crucial in several applications such as machine-to-machine communications, critical telecommunication setup, and backhauling and trunking [2]. Nevertheless, some of these new applications are not economically viable owing to the requirements of the user terminals (UTs) with highly directive tracking antennas. Therefore, there is a commercial interest in small and low-cost UTs for non-geostationary orbit (NGSO) satellite systems based on a wide-beam and low-gain antenna [3]. Since such a small receive antenna will now see multiple NGSO satellites simultaneously, there is an opportunity to combine the signals from these satellites to improve the aggregated data rate, beam load balancing, or enhance the satellite link's robustness through path diversity [4].

However, the lack of phase and time synchronization among multiple satellite paths toward UT results in a misalignment between the received symbols. Consequently, distributed beamforming is extremely challenging [5]. Moreover, in practice, it is hard to obtain accurate channel state information (CSI) at the satellite transmitter. Accordingly, one feasible approach can be to employ space-time block coding (STBC) in satellite communication (SATCOM) systems. As such, the STBC [6] technique can help in achieving the full spatial transmit diversity by sending multiple copies of the same signal, known as space-time codewords, over different signal paths. The other advantage of the STBC scheme is that it does not require fine phase synchronization between the transmitters [7]. Therefore, if the differential phase drift/carrier frequency offset between the two transmitters is kept bound, it will not impact the performance at the UT.

A. Literature Review

As such, the STBC is a very classic topic, and a vast number of research works have been conducted while covering different aspects of the technique. In this respect, the authors in [8] proposed a general linear maximum-likelihood orthogonal STBC (OSTBC) scheme while deriving the closed-form expression of signal-to-noise ratio (SNR) after OSTBC decoding. The impact of a time-varying Rayleigh fading channel on the performance of an Alamouti transmit-diversity scheme was analyzed in [9] while proposing several optimal and sub-optimal detection strategies for mitigating the effects of a time-varying channel. In addition, a dual combining based decoding scheme was proposed to enhance the detection performance of STBC with two transmit antennas in a highly time-varying mobile channel [10]. In some newly published research works, the authors in [11] explored the STBC technique in their analytical framework by considering the imperfect timing offset, however, they have only shown the impact of this impairment on the system performance. Further, the authors in [12] analyzed the STBC-based cooperative relaying system and conducted a measurement campaign.

This work was supported by the European Space Agency (ESA) through the Project DIVERSITY: User Terminal with Path Diversity for Constellations, under activity reference 7B.052 ESA AO/1-10195/20/ITT/15, and the Luxembourg National Research Fund (FNR), through the CORE Project (ARMMONY): Ground-based Distributed Beamforming Harmonization for the Integration of Satellite and Terrestrial Networks, under Grant FNR16352790. (Corresponding author: Vibhum Singh.)

Vibhum Singh, Geoffrey Eappen, Carlos Luis Marcos Rojas, Jorge Luis Gonzalez-Rios, Juan A. Vásquez-Peralvo, Jevgenij Krivochiza, Juan Carlos Merlano-Duncan, Luis Garces Socarras, Symeon Chatzinotas, and Björn Ottersten are with the Interdisciplinary Centre for Security Reliability and Trust (SnT), University of Luxembourg, 1855 Luxembourg City, Luxembourg (e-mail: vibhum.singh@uni.lu).

Wallace A. Martins is with the ISAE-SUPAERO, Université de Toulouse, France.

Rakesh Palisetty is with the Department of Electrical Engineering, Shiv Nadar Institution of Eminence Deemed to be University, Delhi NCR 201314, India.

This article has been accepted for publication in IEEE Communications Letters. This is the author's version which has not been fully edited and content may change prior to final publication. Citation information: DOI 10.1109/LCOMM.2024.3359329

When it comes to non-terrestrial networks, authors in [13] and [14], [15] employed the STBC technique in their analytical frameworks for SATCOM systems and hybrid satellite-terrestrial networks (HSTNs), respectively, while employing heterogeneous fading channel models. Moreover, the authors in [16] discussed the STBC scheme, in particular, Almouti STBC, which deals with time misalignment in the two satellite transmitters while assuming perfect knowledge of the timing offset at the receiver.

B. Motivation and Contributions

Most of the research works relying on STBC transmission are intended for terrestrial networks. On the other hand, SATCOM systems face unique challenges, such as large differential delays among multiple paths and atmospheric attenuation. Moreover, in the downlink/forward (FW) SATCOM system with multiple satellites, the time-misaligned signals from different satellites may produce interference to other waveforms and intersymbol interference (ISI) to own waveform due to the channel characteristics. These challenges make diversity combining schemes particularly important for STBC NGSO SATCOM systems with low-cost UT, as they can help in canceling out the interference experienced by the UT.

Impelled by the preceding discussion, in this letter, we consider a SATCOM system environment including a ground transceiver i.e., UT,[1] that combines the radio-frequency (RF) signals from P NGSO satellites, i.e., MEO or LEO spacecraft, operating in Ka-band, and fed by a gateway (GW) at the ground. The transmitted signals employ STBC encoding. In summary, our main contributions in this letter can be pointed out as follows:

- Considering the time misalignment with respect to each satellite link and appropriately designing the digital receiver structure with multiple branches specifically designed to lock onto each satellite of the multi-satellite system, we formulate a linear model for the UT's received signal vector. Importantly, this receiver structure enables simple UT to operate effectively without increasing the UT's RF complexity.
- As such, the devised linear model includes the extended block matrix while incorporating the interference from multiple satellites. We propose the time-domain zero-forcing (ZF) as a solution to the linear system as a way to perform diversity combining that eliminates or significantly mitigates the interference effects. It is essential to emphasize that the selection of the ZF combiner in this research is unique and employed as an illustrative solution for dealing with timing misalignment. Hereby, we derive the signal-to-interference-plus-noise ratio (SINR) expression at UT.
- Further, we substantiate our analysis through analytical and simulation results. Specifically, we examine the case of Alamouti and propose a novel custom encoding scheme called $\jmath$-$\jmath$ STBC with two NGSO satellites. Our findings showcase the diversity benefits achieved by employing the ZF combiner, leading to significant SINR improvements at the UT. Although $\jmath$-$\jmath$ has been represented differently from Alamouti using complex matrix notation, they exhibit the same performance.

[1]It is noteworthy that the design challenge lies in the requirement for a highly directive and low-cost antenna in the receiver/UT to effectively distinguish among NGSO satellites with required tracking accuracy within densely populated large constellations.

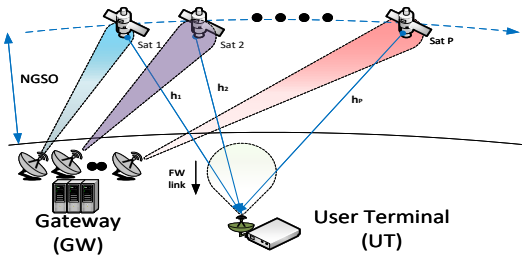

Fig. 1: System model.

- Finally, we extend all the analysis presented in this letter to the minimum mean squared error (MMSE) based combining scheme included in Appendix B. The inclusion of MMSE is particularly relevant, as it is an alternative approach that has the potential to enhance performance.

Mathematical Functions and Notations: We use $\otimes$ to denote the Kronecker product, $\boldsymbol{I}$ to represent the identity matrix, $\mathrm{Tr}(\cdot)$ to express the trace of a matrix, $\mathrm{vec}(\cdot)$ to indicate the vectorization of a matrix, $||\cdot||_{\mathrm{F}}$ to denote the Frobenius norm of a matrix, and $\mathrm{diag}(\cdot)$ to represent the diagonalization of a matrix. Further, $\boldsymbol{R}_{XX} = \mathbb{E}\{\boldsymbol{X}\boldsymbol{X}^{\intercal}\}$ and $\boldsymbol{R}_{XY} = \mathbb{E}\{\boldsymbol{X}\boldsymbol{Y}^{\intercal}\}$ express the auto-covariance and cross-covariance matrices of real-valued random vectors, respectively, with $(\cdot)^{\intercal}$ being the transpose operator.

II. System Description

A. System Model

As depicted in Fig. 1, we consider a SATCOM system environment consisting of P NGSO satellites,[2] each equipped with an antenna array and connected through P highly directive antennas at the GW side. Hereby, we investigate the downlink/FW transmission of linear STBC signals through these NGSO satellites, which are further received by the UT while experiencing the time misalignment of τ_p with respect to each satellite link. Thus, one can define the differential delay between the first two satellite links, e.g., $\tau_d = \tau_1 - \tau_2$. Hereby, we assume that the Doppler variations can be precompensated based on the existing Doppler compensation algorithms [17]. Further, the downlink satellite channel is approximated as the linear additive white Gaussian noise (AWGN) channel [18].

B. Discrete-time Processing

Consider the transmission of K symbols $s[1], s[2], \cdots, s[K] \in \mathscr{C}$ of a symbol constellation $\mathscr{C} \subset \mathbb{C}$ using a linear STBC implemented via GW through P antennas in the field of view of a UT. The K symbols are STBC encoded and transmitted through the P satellites in $T \geq K$ consecutive transmissions. The transmission baud rate is therefore K/T. By denoting the real and imaginary parts of the symbols as $s_{\mathrm{r}}[k] \triangleq \Re\{s[k]\}$ and $s_{\mathrm{i}}[k] \triangleq \Im\{s[k]\}$, respectively, then one can write the STBC encoded signals $\bar{\boldsymbol{s}}_t \triangleq \begin{bmatrix} \bar{s}_t^{(1)} & \cdots & \bar{s}_t^{(P)} \end{bmatrix}^{\intercal}$, with $t \in \mathscr{T} \triangleq \{1, \cdots, T\}$, as

$$\bar{\boldsymbol{S}} = \begin{bmatrix} \bar{\boldsymbol{s}}_1 & \cdots & \bar{\boldsymbol{s}}_T \end{bmatrix} = \sum_{k=1}^{K} \left(s_{\mathrm{r}}[k]\boldsymbol{A}_{\mathrm{r}}[k] + \jmath s_{\mathrm{i}}[k]\boldsymbol{A}_{\mathrm{i}}[k] \right), \quad (1)$$

[2]This scenario can be replicated in a laboratory environment using multiple GW modems, a UT modem, and a multilink satellite channel emulator which is already available at SnT. With this configuration, the communication system can perform the emulation of different orbits and the satellite payload characteristics.

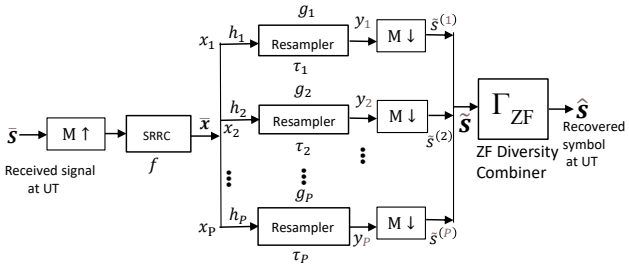

Fig. 2: Receiver structure at UT.

in which $\{\boldsymbol{A}_{\rm r}[k], \boldsymbol{A}_{\rm i}[k]\}_{k=1}^{K}$ are fixed and known code matrices of dimensions $P \times T$. By defining the variables

$$\boldsymbol{A} \triangleq \begin{bmatrix} \boldsymbol{A}_{\rm r}[1] & \jmath\boldsymbol{A}_{\rm i}[1] & \cdots & \boldsymbol{A}_{\rm r}[K] & \jmath\boldsymbol{A}_{\rm i}[K] \end{bmatrix} \in \mathbb{C}^{P\times 2TK}, \quad (2)$$

$$\boldsymbol{s} \triangleq \begin{bmatrix} s_{\rm r}[1] & s_{\rm i}[1] & \cdots & s_{\rm r}[K] & s_{\rm i}[K] \end{bmatrix}^{\intercal} \in \mathbb{R}^{2K\times 1}, \quad (3)$$

then one can rewrite (1) as

$$\bar{\boldsymbol{S}} = \boldsymbol{A} \cdot (\boldsymbol{s} \otimes \boldsymbol{I}_T). \quad (4)$$

Now, the $p^{\rm th}$ satellite, $p \in \mathscr{P} \triangleq \{1, \cdots, P\}$, will transmit the signal $\bar{s}_t^{(p)}$ to the UT at the discrete-time instant $t \in \mathscr{T}$. We shall assume that t is the discrete-time index associated with the symbol sampling time $T_{\rm s} \in \mathbb{R}_+$. The corresponding receiver structure at UT with discrete-time signal processing along with the ZF-based combiner can be illustrated in Fig. 2. After upsampling by a factor $M \in \mathbb{N}$ and digitally pulse-shaping with a square root raised cosine (SRRC) filter $f[n]$,[3] the baseband signal model for the transmitted signal can be written as

$$x_p[n] = \sum_{t\in\mathscr{T}} \bar{s}_t^{(p)} f[n - tM]\,. \quad (5)$$

Let $h_p[n]$ and $g_p[n]$ respectively denote the discrete-time channel model for the link between the UT and the $p^{\rm th}$ payload and the resampling filter response at the $p^{\rm th}$ branch of the UT receiver processing chain, both at the sample rate $M/T_{\rm s}$. Herein, we consider the resampler designed with delay compensation of τ_p with respect to each satellite link which is calculated based on satellite ephemeris. The resampler applies a polynomial timing re-sampler that comprises five possible polynomial coefficients[4], i.e., $c_{-2}, c_{-1}, c_o, c_{+1}, c_{+2}$ [20]. This polynomial resampler is an adaption cubic polynomial re-sampler. The modification used in our actual implementation of the re-sampler allows for handling positive and negative time delays. Thus, the maximum possible differential delay τ_d between two satellite links can be four samples or $\frac{4}{M}$ symbol time.

Now, similar to (3), we consider the original AWGN vector $\boldsymbol{v}$ as

$$\boldsymbol{v} \triangleq \begin{bmatrix} v_{\rm r}[1] & v_{\rm i}[1] & \cdots & v_{\rm r}[K] & v_{\rm i}[K] \end{bmatrix}^{\intercal} \in \mathbb{R}^{2K\times 1}. \quad (6)$$

Hereby, we realize an AWGN vector $\tilde{\boldsymbol{v}}$, $\tilde{\boldsymbol{v}} \in \mathbb{R}^{PT\times 1}$, at receiver after upsampling the original AWGN vector $\boldsymbol{v}$ by the factor M and then passing through it SRRC filter, followed by P parallel resampler chains, each having a delay of τ_p. Consequently, $\tilde{\boldsymbol{v}}$ can be expressed as

$$\tilde{\boldsymbol{v}} = \boldsymbol{Q}\boldsymbol{v}, \quad \text{with } Q = [\boldsymbol{Q}_{\boldsymbol{v}_1}; \boldsymbol{Q}_{\boldsymbol{v}_2}; \cdots, \boldsymbol{Q}_{\boldsymbol{v}_P}], \boldsymbol{Q} \in \mathbb{R}^{PT\times 2KM}, \quad (7)$$

wherein $\boldsymbol{Q}_{\boldsymbol{v}_p}$ denotes the matrix defined for the AWGN while upsampling the original AWGN vector $\boldsymbol{v}$ by the factor M and then passing through it SRRC filter, followed by p-th parallel resampler chain, having a delay of τ_p. Thus, the discrete-time version of the received signal at the $p_0^{\rm th}$ branch of the UT receiver processing chain is

$$\begin{aligned} y_{p_0}[n] &= \sum_{p\in\mathscr{P}} \left(g_{p_0} * f * h_p * x_p\right)[n] + \underbrace{\left(g_{p_0} * f * \tilde{v}\right)[n]}_{\triangleq \tilde{v}_{p_0}[n]} \\ &= \sum_{p\in\mathscr{P}} \sum_{t\in\mathscr{T}} \underbrace{\left(g_{p_0} * f * h_p * f\right)[n - tM]}_{\triangleq \tilde{h}_{p_0,p}[n-tM]} \cdot \bar{s}_t^{(p)} + \tilde{v}_{p_0}[n] \\ &= \sum_{p\in\mathscr{P}} \sum_{t\in\mathscr{T}} \tilde{h}_{p_0,p}[n - tM] \bar{s}_t^{(p)} + \tilde{v}_{p_0}[n]. \end{aligned} \quad (8)$$

Now, after downsampling by factor M, the required output can be written as

$$\begin{aligned} \tilde{s}_{t_0}^{(p_0)} &= y_{p_0}[t_0 M] \\ &= \sum_{p\in\mathscr{P}} \sum_{t\in\mathscr{T}} \underbrace{\tilde{h}_{p_0,p}[(t_0 - t)M]}_{\triangleq c_{p_0,p}^{(t_0,t)}} \cdot \bar{s}_t^{(p)} + \underbrace{\tilde{v}_{p_0}[t_0 M]}_{\triangleq \bar{\tilde{v}}_{t_0}^{(p_0)}} \\ &= \sum_{p\in\mathscr{P}} \sum_{t\in\mathscr{T}} c_{p_0,p}^{(t_0,t)} \cdot\ \bar{s}_t^{(p)} + \bar{\tilde{v}}_{t_0}^{(p_0)}\,. \end{aligned} \quad (9)$$

By defining $\tilde{\boldsymbol{s}}_t \triangleq \begin{bmatrix} \tilde{s}_t^{(1)} & \cdots & \tilde{s}_t^{(P)} \end{bmatrix}^{\intercal} \in \mathbb{C}^{P\times 1}$, $\bar{\tilde{\boldsymbol{v}}}_t \triangleq \begin{bmatrix} \bar{\tilde{v}}_t^{(1)} & \cdots & \bar{\tilde{v}}_t^{(P)} \end{bmatrix}^{\intercal} \in \mathbb{C}^{P\times 1}$, with $t \in \mathscr{T}$, and

$$\tilde{\bar{\boldsymbol{s}}} \triangleq \begin{bmatrix} \tilde{\boldsymbol{s}}_1^{\intercal} & \cdots & \tilde{\boldsymbol{s}}_T^{\intercal} \end{bmatrix}^{\intercal} \in \mathbb{C}^{PT\times 1}, \quad (10)$$

$$\bar{\tilde{\boldsymbol{v}}} \triangleq \begin{bmatrix} \bar{\tilde{\boldsymbol{v}}}_1^{\intercal} & \cdots & \bar{\tilde{\boldsymbol{v}}}_T^{\intercal} \end{bmatrix}^{\intercal} \in \mathbb{C}^{PT\times 1}, \quad (11)$$

$$\bar{\boldsymbol{s}} \triangleq \mathrm{vec}(\bar{\boldsymbol{S}}) \in \mathbb{C}^{PT\times 1}, \quad (12)$$

then, from (9), one can write

$$\tilde{\bar{\boldsymbol{s}}} = \boldsymbol{C}\bar{\boldsymbol{s}} + \bar{\tilde{\boldsymbol{v}}}\,, \quad (13)$$

where the matrix $\boldsymbol{C} \in \mathbb{C}^{PT\times PT}$ has entries defined as

$$[\boldsymbol{C}]_{p_1+(t_1-1)P, p_2+(t_2-1)P} \triangleq c_{p_1,p_2}^{(t_1,t_2)}\,, \quad (14)$$

for all $p_1, p_2 \in \mathscr{P}$ and for all $t_1, t_2 \in \mathscr{T}$. Thus, (13) can be rewritten as

$$\begin{aligned} \tilde{\bar{\boldsymbol{s}}} &= \boldsymbol{C} \cdot \mathrm{vec}\left(\boldsymbol{A} \cdot (\boldsymbol{s} \otimes \boldsymbol{I}_T)\right) + \bar{\tilde{\boldsymbol{v}}} \\ &= \boldsymbol{C} \cdot (\boldsymbol{I}_T \otimes \boldsymbol{A}) \cdot \mathrm{vec}(\boldsymbol{s} \otimes \boldsymbol{I}_T) + \bar{\tilde{\boldsymbol{v}}}\,. \end{aligned} \quad (15)$$

Let $\boldsymbol{\alpha}_{2T^2K}^{(i)}$ be the $i^{\rm th}$ column of the $2T^2K$-dimension identity matrix $\boldsymbol{I}_{2T^2K}$, with $i \in \{1, \cdots, 2T^2K\}$. In addition, let us define the $2T^2K \times 2K$ matrix $\boldsymbol{B}$ with the $j^{\rm th}$ column, $\boldsymbol{b}_j$, defined as follows:

$$\boldsymbol{b}_j \triangleq \sum_{t\in\mathscr{T}} \boldsymbol{\alpha}_{2T^2K}^{(1+(t-1)T+(j-1)T^2)}\,,\ \forall j \in \{1, \cdots, 2K\}\,. \quad (16)$$

Note that the resulting columns of $\boldsymbol{B}$ are orthogonal. With these definitions, one has

$$\mathrm{vec}(\boldsymbol{s} \otimes \boldsymbol{I}_T) = \boldsymbol{B} \cdot \boldsymbol{s}\,, \quad (17)$$

[3]Note that n is the discrete-time index at a sampling frequency $M/T_{\rm s}$.

[4]The employed resampler takes the form of an FIR filter featuring variable coefficients. In contrast to alternative digital resampling methods such as filter banks, polynomial resamplers present a simpler control structure. This structure is based on a single input parameter, rendering it more appealing for real-time applications implemented in hardware [19].

This article has been accepted for publication in IEEE Communications Letters. This is the author's version which has not been fully edited and content may change prior to final publication. Citation information: DOI 10.1109/LCOMM.2024.3359329

thus, from (15), and thereby invoking the value of $\bar{\bar{\boldsymbol{v}}}$ from (7), one gets

$$\begin{aligned}\tilde{\boldsymbol{s}} &= \underbrace{\boldsymbol{C}\cdot(\boldsymbol{I}_T\otimes\boldsymbol{A})\cdot\boldsymbol{B}}_{\triangleq\boldsymbol{D}\,\in\,\mathbb{C}^{PT\times 2K}}\cdot\boldsymbol{s}+\bar{\bar{\boldsymbol{v}}}\\ &= \boldsymbol{D}\cdot\boldsymbol{s}+\boldsymbol{Q}\bar{\boldsymbol{v}},\end{aligned} \tag{18}$$

wherein $\boldsymbol{D}$ being the extended block matrix while incorporating the interference from multiple satellites at UT. Hereby, we can define an estimator that will play the role of the combiner in the proposed architecture.

III. Combiner Design

Herein, considering the model in (18), we define the simple linear ZF combiner denoted as $\boldsymbol{\Gamma}_{\text{ZF}}$. In this case, one can obtain a soft estimate $\hat{\boldsymbol{s}}\in\mathbb{C}^{2K\times 1}$ of the symbols via

$$\begin{aligned}&\hat{\boldsymbol{s}}=\boldsymbol{\Gamma}_{\text{ZF}}\,\tilde{\boldsymbol{s}},\\ &\text{with }\boldsymbol{\Gamma}_{\text{ZF}}=\left(\boldsymbol{D}^{\text{H}}\boldsymbol{D}\right)^{-1}\boldsymbol{D}^{\text{H}},\boldsymbol{\Gamma}_{\text{ZF}}\in\mathbb{C}^{2K\times PT}.\end{aligned} \tag{19}$$

Thus, the theoretical output SINR at UT for the ZF combiner can be provided with the help of Theorem 1 as given below.

Theorem 1: The theoretical output SINR for the ZF combiner can be computed as

$$\text{SINR}_{\text{ZF}}=10\log_{10}\left(\frac{\sigma_s^2}{\sigma_v^2}\right)-10\log_{10}\left(\frac{\|\boldsymbol{\Gamma}_{\text{ZF}}Q\|_{\text{F}}^2}{2K}\right), \tag{20}$$

with σ_s^2 and σ_v^2 denote the corresponding variances for the complex-valued symbols and AWGN vector.

Proof: See Appendix A. ∎

Remark 1: Since $\boldsymbol{D}$ is $PT\times 2K$, with $P\geq 2$ and $T\geq K$, it is possible to conveniently define the processing operations at transmitter and receiver sides so that matrix $\boldsymbol{D}$ has full column rank, thus guaranteeing the existence of the inverse of matrix $\boldsymbol{\varphi}=\boldsymbol{D}^{\text{H}}\boldsymbol{D},\in\mathbb{C}^{2K\times 2K}$.

Remark 2: In particular, we calculate the condition number for this φ in the numerical results section, where the finite condition number ensures the inverse of the matrix φ and results in the recovered transmitted symbols at UT. Importantly, we employ the properties of block circulant matrix for efficient computation of the inverse of the matrix $\boldsymbol{\varphi}$, and consequently multiplication operation in $\boldsymbol{\Gamma}_{\text{ZF}}$ [21].

IV. Numerical and Simulation Results

For numerical results, we set $K=1024, T=2K, M=4, T_s=1$. In particular, we draw all the figures while setting $P=2$, and thus, $\tau_d=|\tau_1-\tau_2|$. Hereby, two encoding schemes have been considered, viz., Alamouti and $\jmath$-$\jmath$. The corresponding encoder matrices can be represented in a real stacked representation as the concatenation of the real and imaginary parts of the encoders as

$$a_0=\begin{bmatrix}1&0&0&0\\0&1&0&0\\0&0&-1&0\\0&0&0&1\end{bmatrix},\quad a_1=\begin{bmatrix}0&0&1&0\\0&0&0&1\\1&0&0&0\\0&-1&0&0\end{bmatrix},$$

$$a_0=\begin{bmatrix}1&0&0&0\\0&1&0&0\\0&0&0&1\\0&0&-1&0\end{bmatrix},\quad a_1=\begin{bmatrix}0&0&1&0\\0&0&0&1\\0&-1&0&0\\1&0&0&0\end{bmatrix}.$$

The above real-valued representations help to write the encoding matrices properly as a linear operation. Further, for notation simplicity, we denote resampler with delay compensation and resampler without delay compensation as Compensated and Non-Compensated, respectively.

Fig. 3(a) illuminates the simulation curves for the condition number of φ versus differential delay τ_d under the setting of various values of h_1 and h_2. From the figure, one can note the increase in the condition number as the value of τ_d increases. Also, the changes in values of the channels' phase provide the same condition number. Further, we explicitly designed our resampler with delay compensation to ensure a finite condition number, as described earlier. Its impact can be shown in the improvement in SINR at UT in the next sub-figure.

Fig. 3(b) depicts the SINR versus τ_d curves for Alamouti encoding under the various values of noise amplitudes v_{amp}. For this, we set $h_1=1, h_2=\exp\left(j\frac{\pi}{2}\right)$. Further, for comparison purposes, we have drawn the simulation curves for non-compensated ones. First, it can be ensured that the analytical curves are well matched with the exact simulation result. As such, it can be seen that SINR decreases as the value of τ_d increases. However, its adverse effect is more proned when considering the non-compensated approach.

Fig. 3(c) demonstrates the SINR versus τ_d curves for $\jmath$-$\jmath$ encoding under the various values of v_{amp}. From the figure, one can note that both Alamouti and $\jmath$-$\jmath$ exhibit almost the same performance with respect to received SINR at UT. The similarity in performance can be justified by examining the linear operations involved in their processing, as well as the common principles underlying STBC and the ZF combiner.

V. Conclusion

In this letter, we investigated the downlink transmission of linear STBC signals from multiple geographically distributed NGSO satellites. Considering the practical time misalignment with respect to each satellite link and accordingly designing the digital receiver structure with multiple branches specifically designed to lock onto each satellite of the multi-satellite system at UT, we formulated a linear model for the received signal vector. As such, the devised linear model includes the extended block matrix while incorporating interference from multiple satellites. To address this issue, a ZF-based diversity combining scheme was proposed. Our results demonstrated the SINR improvement at UT achieved by the ZF combiner. For future work, it would be fascinating to explore the performance with ZF combiner/equalizer while invoking the Doppler frequency shift in the channel.

Appendix A

Referring to (19), the mean squared error (MSE) associated with the ZF combiner and averaged across the $2K$ entries can be computed as

$$\begin{aligned}\mathscr{E}_{\text{ZF}}=&\frac{1}{2K}\mathbb{E}\left\{\|\boldsymbol{s}-\boldsymbol{\Gamma}_{\text{ZF}}\tilde{\boldsymbol{s}}\|^2\right\}\\ =&\frac{1}{2K}\text{Tr}\left\{\boldsymbol{R}_{ss}-\boldsymbol{\Gamma}_{\text{ZF}}\boldsymbol{R}_{\tilde{s}s}-\boldsymbol{R}_{s\tilde{s}}\boldsymbol{\Gamma}_{\text{ZF}}^{\text{H}}+\boldsymbol{\Gamma}_{\text{ZF}}\boldsymbol{R}_{\tilde{s}\tilde{s}}\boldsymbol{\Gamma}_{\text{ZF}}^{\text{H}}\right\}.\end{aligned} \tag{21}$$

Let us assume that the transmitted complex-valued symbols and complex-valued noise are the realizations of *independent and*

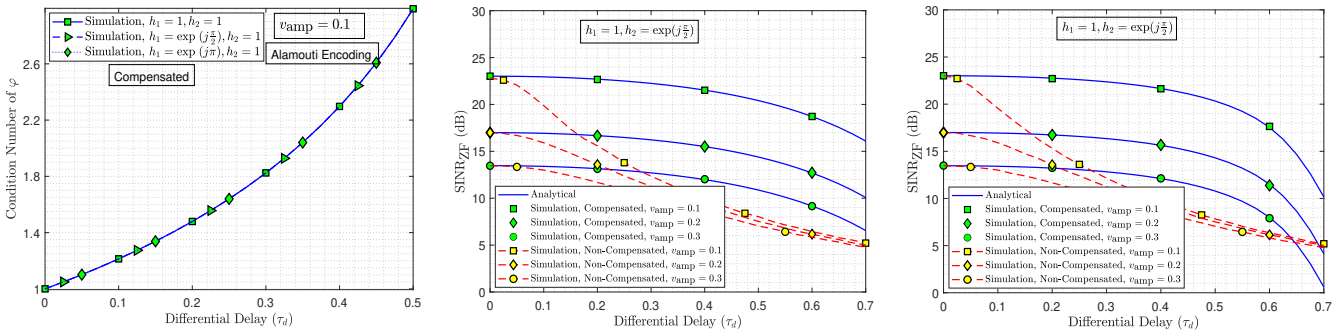

(a) (b) (c)

Fig. 3: (a) Condition number of φ versus differential delay curves; (b) SINR versus differential delay curves for Alamouti encoding; (c) SINR versus differential delay curves for $\jmath$-$\jmath$ encoding.

identically distributed (i.i.d.) random variables with zero mean and variances σ_s^2 and σ_v^2, respectively, wherein the corresponding real and imaginary parts contribute equally to the variances ($\sigma_s^2/2$ each) and ($\sigma_v^2/2$ each). Further, assuming that symbol and noise are uncorrelated, i.e., $\mathbb{E}\{\boldsymbol{s}\boldsymbol{v}^\intercal\} = \mathbf{0}_{2K\times 8K}$, then one has

$$\begin{aligned}
\boldsymbol{R}_{ss} &= \mathbb{E}\{\boldsymbol{s}\boldsymbol{s}^\intercal\} = \frac{\sigma_s^2}{2}\boldsymbol{I}_{2K}, \boldsymbol{R}_{\tilde{s}s} = \mathbb{E}\{\tilde{\boldsymbol{s}}\boldsymbol{s}^\intercal\} = \frac{\sigma_s^2}{2}\boldsymbol{D}, \\
\boldsymbol{R}_{s\tilde{s}} &= \mathbb{E}\{\boldsymbol{s}\tilde{\boldsymbol{s}}^\intercal\} = \frac{\sigma_s^2}{2}\boldsymbol{D}^{\text{H}}, \\
\boldsymbol{R}_{\tilde{s}\tilde{s}} &= \mathbb{E}\{\tilde{\boldsymbol{s}}\tilde{\boldsymbol{s}}^\intercal\} = \frac{\sigma_s^2}{2}\boldsymbol{D}\boldsymbol{D}^{\text{H}} + \frac{\sigma_v^2}{2}\boldsymbol{Q}\boldsymbol{Q}^\intercal. \qquad (22)
\end{aligned}$$

Hereby, on invoking (22) into (21), and simplifying further with the help of (19), one gets the MSE for ZF combiner as

$$\mathscr{E}_{\text{ZF}} = \frac{\sigma_v^2}{2K\sigma_s^2}\text{Tr}\left\{\boldsymbol{\Gamma}_{\text{ZF}}\boldsymbol{Q}\boldsymbol{Q}^\intercal\boldsymbol{\Gamma}_{\text{ZF}}^{\text{H}}\right\} = \frac{\sigma_v^2}{2K\sigma_s^2}\left\|\boldsymbol{\Gamma}_{\text{ZF}}Q\right\|_{\text{F}}^2. \qquad (23)$$

Thus, the theoretical output SINR for the ZF combiner can be computed as

$$\text{SINR}_{\text{ZF}} = -10\log_{10}\left(\mathscr{E}_{\text{ZF}}\right). \qquad (24)$$

Finally, on substituting the $\mathscr{E}_{\text{ZF}}$ from (23), one can grab the desired result in (20).

Appendix B

Herein, we extend our analysis presented in this letter to the MMSE combiner case. Thus, referring to (19), one can obtain a soft estimate $\hat{\boldsymbol{s}} \in \mathbb{C}^{2K\times 1}$ of the symbols via

$$\begin{aligned}
&\hat{\boldsymbol{s}} = \boldsymbol{\Gamma}_{\text{MMSE}}\,\tilde{\boldsymbol{s}}, \\
&\text{with } \boldsymbol{\Gamma}_{\text{MMSE}} = \boldsymbol{D}^{\text{H}}\left(\boldsymbol{D}\boldsymbol{D}^{\text{H}} + \frac{\sigma_v^2}{\sigma_s^2}\boldsymbol{Q}\boldsymbol{Q}^\intercal\right)^{-1}. \qquad (25)
\end{aligned}$$

Now, by invoking (18) into (25), one can write

$$\begin{aligned}
\hat{\boldsymbol{s}} &= \boldsymbol{\Gamma}_{\text{MMSE}}\boldsymbol{D}\boldsymbol{s} + \boldsymbol{\Gamma}_{\text{MMSE}}\boldsymbol{Q}\bar{\boldsymbol{v}} \\
&= \boldsymbol{\Upsilon}\boldsymbol{s} + \boldsymbol{\Gamma}_{\text{MMSE}}\boldsymbol{Q}\bar{\boldsymbol{v}}, \qquad (26)
\end{aligned}$$

with $\boldsymbol{\Upsilon} = \boldsymbol{\Gamma}_{\text{MMSE}}\boldsymbol{D}$. Now, (26) can be re-expressed as

$$\hat{\boldsymbol{s}} = \underbrace{\text{diag}\{\boldsymbol{\Upsilon}\}\,\boldsymbol{s}}_{\text{desired signal}} + \underbrace{\left(\boldsymbol{\Upsilon} - \text{diag}\{\boldsymbol{\Upsilon}\}\right)\boldsymbol{s}}_{\text{interference}} + \underbrace{\boldsymbol{\Gamma}_{\text{MMSE}}\boldsymbol{Q}\bar{\boldsymbol{v}}}_{\text{noise}}. \qquad (27)$$

Hereby, after some manipulation, one can get the desired output SINR for the MMSE combiner as

$$\begin{aligned}
\text{SINR}_{\text{MMSE}} &= 10\log_{10}\left(\frac{\sigma_s^2}{\sigma_v^2}\right) \\
&- 10\log_{10}\left(\frac{\frac{\sigma_s^2}{\sigma_v^2}\left\|\boldsymbol{\Upsilon} - \text{diag}\{\boldsymbol{\Upsilon}\}\right\|_{\text{F}}^2 + \left\|\boldsymbol{\Gamma}_{\text{MMSE}}\boldsymbol{Q}\right\|_{\text{F}}^2}{\left\|\text{diag}\{\boldsymbol{\Upsilon}\}\right\|_{\text{F}}^2}\right). \qquad (28)
\end{aligned}$$

References

[1] *Transcending Connectivity*, SES, Betzdorf, Luxembourg, Sep. 2017.

[2] O. Kodheli *et*. al, "Satellite communications in the new space era: A survey and future challenges," *IEEE Commun. Surv. Tut.*, vol. 23, no. 1, pp. 70-109, Oct. 2020.

[3] J. A. Vásquez-Peralvo *et*. al, "Wide-beamwidth circular polarized antenna for diversity combining applications," in *Proc. IEEE Globecom Workshops (GC Wkshps)*, Rio de Janeiro, Brazil, Dec. 2022, pp. 1395-1399.

[4] D. Gesbert, M. Shafi, D. Shiu, P. J. Smith, and A. Naguib, "From theory to practice: An overview of MIMO space–time coded wireless systems," *IEEE J. Sel. Areas Commun.*, vol. 21, no. 4, pp. 281-302, Apr. 2003.

[5] R. Mudumbai, D. R. Brown Iii, U. Madhow, and H. V. Poor, "Distributed transmit beamforming: Challenges and recent progress," *IEEE Commun. Mag.*, vol. 47, no. 2, pp. 102-110, Feb. 2009.

[6] S. M. Alamouti, "A simple transmit diversity technique for wireless communications," *IEEE J. Sel. Areas Commun.*, vol. 16, no. 8, pp. 1451-1458, Oct. 1998.

[7] Y. Dhungana, N. Rajatheva, and C. Tellambura, "Dual hop MIMO OSTBC for LMS communication," *IEEE Wireless Commun. Lett.* , vol. 1, no. 2, pp. 105-108, Apr. 2012.

[8] X. Li, T. Luo, G. Yue, and C. Yin, "A squaring method to simplify the decoding of orthogonal space–time block codes," *IEEE Trans. Commun.*, vol. 49, no. 10, pp. 1700-1703, Oct. 2001.

[9] A. Vielmon, Y. (G.) Li, and J. R. Barry, "Performance of Alamouti transmit diversity over time-varying Rayleigh-fading channels," *IEEE Trans. Wireless Commun.*, vol. 3, no. 5, pp. 1369-1373, Sep. 2004.

[10] J. Wee, W. Jeon, K. Park, H. Kim, and Y. Cho, "A dual combining based decoding scheme for two-branched mobile STBC," *IEEE Trans. Consumer Electronics*, vol. 54, no. 4, pp. 1635-1639, Nov. 2008.

[11] M. W. Akhtar, S. A. Hassan, S. Saleem, and H. Jung, "STBC-aided cooperative NOMA with timing offsets, imperfect successive interference cancellation, and imperfect channel state information," *IEEE Trans. Veh. Technol.*, vol. 69, no. 10, pp. 11712-11727, Oct. 2020.

[12] H. Murata, A. Kuwabara, and Y. Oishi, "Distributed cooperative relaying based on space-time block code: System description and measurement campaign," *IEEE Access*, vol. 9, pp. 25623-25631, Feb. 2021.

[13] R. He and Z. Shen, "System design and performance of ship-borne satellite high-speed data reliable transportation based on coded STBC-OFDM," in *Proc. 2022 7th Int. Conf. Intelligent Computing and Sig. Processing (ICSP)*, Xi'an, China, 2022, pp. 1302-1306.

[14] M. Toka, M. Vaezi and W. Shin, "Outage analysis of Alamouti-NOMA scheme for hybrid satellite-terrestrial relay networks," *IEEE Internet of Things Journ.*, vol. 10, no. 6, pp. 5293-5303, Mar. 2023.

[15] V. Singh *et* al., "On the performance of cache-free/cache-aided STBC-NOMA in cognitive hybrid satellite-terrestrial networks," *IEEE Wireless Commun. Lett.*, vol. 11, no. 12, pp. 2655-2659, Dec. 2022.

[16] A. Modenini, A. Ugolini, A. Piemontese, and G. Colavolpe, "On the use of multiple satellites to improve the spectral efficiency of broadcast transmissions," *IEEE Trans. Broadcast.*, vol. 61, no. 4, pp. 590-602, Dec. 2015.

[17] A. K. Meshram, S. Kumar, J. Querol, S. Chatzinotas, "Doppler effect mitigation in LEO-based 5G non-terrestrial networks," in *Proc. IEEE Global Commun. Conf. (GLOBECOM)*, Kuala Lumpur, Malaysia, Dec. 2023, pp. 1-6.

[18] D. Christopoulos, S. Chatzinotas, and B. Ottersten, "User scheduling for coordinated dual satellite systems with linear precoding," in *Proc. IEEE Int. Conf. Commun. (ICC)*, Budapest, Hungary, Jun. 2013, pp. 4498–4503.

[19] Fuyun Ling, "Synchronization in digital communication systems," *Cambridge University Press*, 2017.

[20] U. Mengali and A. N. D'Andrea, "Synchronization techniques for digital receivers," 1997.

[21] R. Vescovo, "Inversion of block-circulant matrices and circular array approach," *IEEE Trans. Antennas Prop.*, vol. 45, no. 10, pp. 1565-1567, Oct. 1997.